PHILOSOPHICAL TRANSACTIONS A

Phil. Trans. R. Soc. A.
doi:10.1098/not yet assigned

# New nitrides: from high pressure-high temperature synthesis to layered nanomaterials and energy applications

**Paul F. McMillan**[1]

[1]*Department of Chemistry, Christopher Ingold Laboratories, University College London, London WC1H 0AJ, UK*

**Keywords:** metal nitride, high pressure, carbon nitride, synchrotron X-ray diffraction, spectroscopy, nanomaterials, exfoliation, PEM fuel cells

## Summary

We describe work carried out within our group to explore new transition metal and main group nitride phases synthesised using high pressure-high temperature techniques using X-ray diffraction and spectroscopy at synchrotron sources in the US, UK and France to establish their structures and physical properties. Along with previously published data we also highlight additional results that have not been presented elsewhere and that represent new areas for further exploration. We also describe new work being carried out to explore the properties of carbon nitride materials being developed for energy applications and the nature of few-layered carbon nitride nanomaterials with atomically ordered structures that form solutions in polar liquids *via* thermodynamically driven exfoliation.

## Introduction

Nitride materials form an important class of solid state compounds with useful functional properties, ranging from refractory ceramics such as $Si_3N_4$ and AlN, to (Ga,In,Al)N wide-gap semiconductors, high-$T_c$ superconductors (NbN) and high-hardness metallic nitrides (MoN, TiN), that are also useful catalysts. However, despite major advances made over the past two decades, the field of nitride solid state chemistry remains under-explored compared with that of oxide materials (1-3). Transition metal nitrides tend to form compounds dominated by intermetallic bonding and they do not typically achieve the highest oxidation states found among corresponding oxide compounds (e.g., TiN *vs* $TiO_2$; MoN *vs* $MoO_3$ etc). Researchers have applied various chemical synthesis and physical vapor deposition techniques, as well as high pressure-high temperature (HPHT) approaches to explore and attempt to achieve novel nitride phases with higher nitrogen:metal (N:M) contents (1). These studies have been greatly facilitated by synchrotron X-ray diffraction, as well as by neutron scattering techniques to investigate the progress of the reactions and the structures formed. Work on main group nitrides has focused on materials and compounds formed with groups 13-15 elements including Si, Ge and Ga, that give rise to wide-gap semiconducting ceramics (2). Here synchrotron X-ray diffraction and investigations of the electronic structure using X-ray absorption and emission measurements combined with *ab initio* theoretical calculations have been key to exploring and establishing the optoelectronic properties of this potentially important family of materials. Studies designed to produce new $sp^3$-bonded forms of the hypothetical carbon nitride $C_3N_4$ were motivated by theoretical predictions that an ultra-low compressibility phase with "superhard" properties possibly competitive with diamond might exist (4, 5). Despite many studies combining HPHT synthesis with synchrotron X-ray diffraction and spectroscopy, formation of this phase remains elusive. However, the related $sp^3$-bonded $C_2N_2H$ phase formed at HPHT followed by its recovery to ambient conditions was established using synchrotron XRD, combined with *ab*

*Author for correspondence (p.f.mcmillan@ucl.ac.uk).
†Present address: Department of Chemistry, Christopher Ingold Laboratories, 20 Gordon Street, London WC1H 0AJ, UK

*initio* theory and laboratory spectroscopy experiments (6, 7). In other work, compression studies carried out on the layered polytriazine imide (PTI) phase $C_2N_3H_3$.HCl showed that layer buckling accompanied by interlayer C-N bonding occurs at high pressure, leading to a new family of pillared-layered solids (8). Laser heating samples of the recently reported graphitic $C_3N_4$ compressed to 40 GPa has led to a new family of open-framework structures with mixed $sp^2/sp^3$ bonding, identified using *ab initio* random structure searching (AIRSS) methods (9, 10), opening up a new area in carbon nitride solid state chemistry. Layered to polymeric carbon nitrides prepared at near-ambient conditions show potential for intercalating $Li^+$ ions or anchoring electrocatalytically active Pt and other metal nanoparticles, for energy storage and conversion applications (11-14). Studies of the oxidation state changes and charge transfer processes involving the catalytic nanoparticles and their interactions with the support materials are now being investigated using *in situ/operando* X-ray scattering under electrochemical test conditions. Crystalline PTI-structured carbon nitride samples are also being studied using a combination of X-ray and neutron scattering, leading to detailed analysis of the local and extended range structures. These crystalline PTI phases undergo spontaneous exfolation and dissolution into polar solvents, producing few-layer g-$C_xN_y$ nanosheets as "inks" that can then be evaporated and deposited as crystalline nanodots with variable layer stacking on different surfaces (15-17). The dissolution mechanisms and structure of the nanomaterials in solution, as well as of the re-deposited nanoflakes, are now being investigated using synchrotron X-ray and neutron scattering techniques, combined with *ab initio* calculations. Here we describe some of the work we have carried out on these nitride systems, using synchrotron sources ranging from Brookhaven NSLS and Daresbury SLS, to Diamond Light Source, ESRF and APS. We highlight some of the results we obtained initially at the "2G" instruments, that became significantly improved when we began to access "3G" sources with enhanced sample environment and experimental capabilities. Here we note some intriguing preliminary results that have been presented in PhD theses from our UCL group that point to new areas for future exploration. As we enter a period of major upgrades to existing synchrotron sources to improve their brightness, reduce the volume sampled to nanoscale dimensions and enable new types of diffraction, imaging and spectroscopic experiments, we expect that a new generation of studies will reveal presently unsuspected structures, functional properties and chemical reactivity. Associating these studies with new capabilities to investigate small samples held under extreme high-P conditions using neutron diffraction and scattering techniques will particularly expand the range of our understanding of the structures and dynamics of these compounds that often incorporate light elements along with high-Z metal atoms. Finally, new "4G" free-electron laser (FEL) light sources developed both as large national or international facilities, or in laboratory-scale environments, provide a high degree of spatial and temporal coherence that will permit new studies of structural transformations, reaction dynamics and physical property responses to external stimuli on a femtosecond to sub-fs timescale ((18-25).

## Transition Metal Nitrides

The main families of transition metal nitrides along with corresponding carbides and carbonitride solid solutions form highly refractory, high hardness metallic materials that often have sub-stoichiometric as well as variable metal/nitrogen (M/N) ratios. These materials have applications as abrasives and for their electronic properties, including high-$T_c$ superconductivity, as well as catalytic activity. NbN achieves $T_c$ = 17K and is used in superconducting coils and antenna devices. It has been predicted that a corresponding γ-MoN phase with the cubic rocksalt structure might achieve $T_c$ values up to ~30K, and there have been many attempts to prepare and characterise such a material. However, the limiting composition found in most studies to date has been close to $MoN_{0.5}$, consistent with theoretical predictions that the fully stoichiometric rocksalt structure would be dynamically unstable (26, 27). Samples of the cubic phase synthesized using high-P,T techniques were shown to achieve $T_c$ values up to ~5K depending on the ordering pattern of N-site vacancies, studied using a combination of X-ray and neutron diffraction (26-29). However, recent results suggest that a cubic phase with 1:1 stoichiometry might be formed, perhaps stabilised by magnetic ordering effects (30). The well known stoichiometric δ-MoN phase adopts a hexagonal layered structure, that achieves $T_c$ values between 4-15K, depending on ordering of the N atoms on the anion sites (31). Other Mo-N phases with stoichiometries extending up to $MoN_2$ have been reported, including from high-P,T synthesis reactions (1, 32). Several of these compounds have been reported to be useful for hydrogenation catalysis (32). In future work it will be useful to explore the N stoichiometry and ordering behaviour of cubic and hexagonal phases using a combination of synchrotron X-ray and neutron diffraction including *in situ* following high-P,T synthesis and during recovery, to establish correlations between the structures and synthesis conditions, and the superconducting and catalytic properties.

We used synchrotron X-ray diffraction in the diamond anvil cell to investigate the compressibilities of several high hardness nitrides (33, 34)). Because of the low compressibility values it is often thought essential to measure the diffraction patterns and unit cell parameters of such phases over a wide pressure range to obtain

reliable V(P) fits (33). However, the P-V data are readily transformed into the corresponding Eulerian stress ($F$) and finite strain ($f_v$) variables:

$$f_v = \frac{1}{2}\left[\left(\frac{V}{V_0}\right)^{-2/3} - 1\right]$$

$$F = P\left(3f(1+2f)^{5/2}\right)^{-1}$$

The resulting $F(f)$ plot reveals a linear relationship with intercept as $F \rightarrow 0$ at the value of $K_v$, the zero pressure bulk modulus (or $K_v$, if the reference volume is taken at another pressure (35, 36)) and slope $K_0'$, its pressure derivative (that is typically approximated to a value of 4, in a third-order Birch-Murnaghan fitting procedure to the non-linear V(P) relation). The $F$-$f$ plot relies mainly on high quality data obtained in the lower pressure regime, that is an advantage for experimental studies. It also reveals the presence of underlying phase transitions or other structural transformation events, that can be difficult to detect from a non-linear $P$-$V$ plot of the compressibility data (35, 36). During compression studies of powdered or polycrystalline samples of mechanically resistant materials, it is important to recognise that the stress-strain relations within individual grains or structural domains may be mainly imposed by intergrain contacts, rather than the hydrostatic qualities of the pressure-transmitting medium, and this may lead to anomalously high bulk modulus values (33). In our angle-dispersive synchrotron XRD study of ε-TaN compressed in NaCl we observed broadening of the diffraction peaks occurring above 10-15 GPa, that could have been due to non-isotropic strains caused by this effect. However, the diffraction lines for small crystals of Au mixed intimately with the sample and used as a pressure standard did not show any broadening, and it was suggested that perhaps some structural disordering process was occurring within the ε-TaN crystal lattice (33).

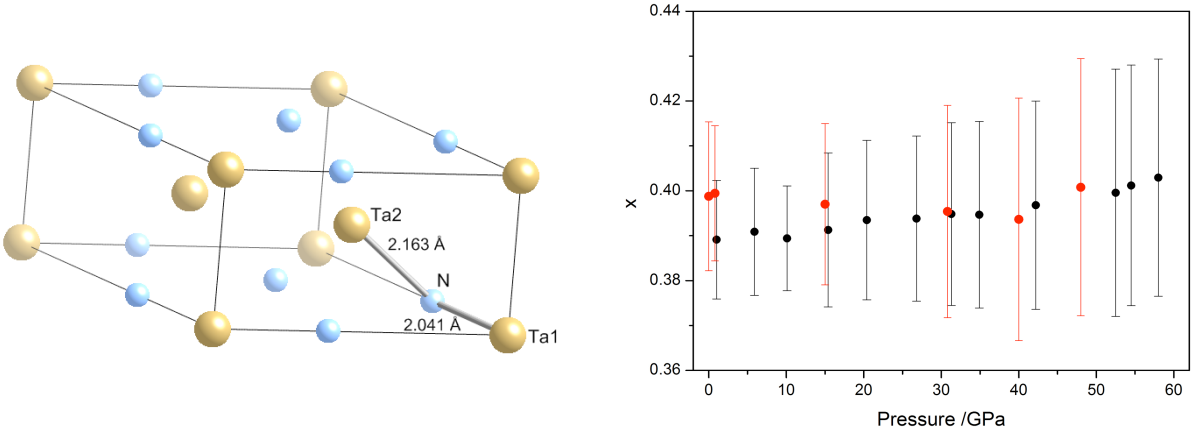


**Figure 1.** Left: A drawing of the ε-TaN unit cell with Ta atoms represented by tan spheres and N atoms as blue spheres. The Ta atoms occupy sites with $D_{3h}$ (Ta1) and $C_{3h}$ (Ta2) symmetry (left). The N positions can be displaced along the Ta1...Ta1 vectors with no change in unit cell symmetry. The Ta1 and Ta2 distances to the N atoms are given for the ambient pressure structure. Right: Changes in the fractional position (x) of the N atoms along the *a* axis during compression (black) and decompression (red). Diagrams adapted from the PhD thesis of Katherine Woodhead (UCL) (ref. (37)).

Raman spectroscopic data collected up to 58 GPa revealed an unexpected crossover in the ν($P$) relations for the Ta-N stretching modes at ~20 GPa, suggesting the possibility of a displacive event involving the N atom positions (33). The ε-TaN structure has $P\bar{6}2m$ symmetry with Ta atoms on 1*a* ($D_{3h}$) and 2*d* ($C_{3h}$) Wyckoff sites, and N atoms on *3f* ($C_{2v}$) positions. Within the unit cell, the N positions along the *a* axis direction are not constrained by symmetry and could re-adjust during compression. However, X-ray diffraction data do not give information on the N atom positions because of the much stronger scattering from the high-Z metal atoms. We investigated this problem using energy-dispersive X-ray absorption (XAS) with analysis of the extended X-ray absorption fine structure (EXAFS) data at ESRF beamline ID24 (37, 38). Modelling the results using selected Ta...N scattering paths showed that the N atomic positions along the *a* axis changed during compression to reach a fractional coordinate 0.401 by 35 GPa, that had still not achieved an ideal value of 0.5 in the centre of the unit cell adge defined by Ta...Ta distances (Fig. 1). That observation supports the idea that broadening in the XRD data could be associated with internal disorder within the structure, associated with variability in the Ta-N bond lengths, and resulting lowered change in the first-shell Ta-N distances with pressure might contribute to the anomalous behaviour of the Ta-N stretching frequencies. This work that was

described in the PhD thesis of K.E. Woodhead (37) indicates how high pressure XAS/EXAFS, XRD and Raman scattering data can be usefully combined to identify and address structural problems including local site ordering in systems containing a mixture of high- and low-Z elements, in a high pressure range that is only beginning to be accessible to neutron scattering studies (35).

In 1999, independent studies using synchrotron X-ray diffraction and Raman spectroscopy first revealed the cubic spinel-structured (γ-) polymorphs of the ceramic phases $Si_3N_4$ and $Ge_3N_4$ (39, 40). These constituted the first examples of the new class of nitride spinels, that were soon joined by the remaining group 14 member $Sn_3N_4$, initially prepared by chemical reaction techniques at near-ambient conditions (41) and later by HPHT synthesis (42). The new nitride spinels have potentially useful optoelectronic properties including wide, direct bandgaps in the blue-UV range, comparable with (Ga,In,Al)N solid solutions (43-45). The first observations of γ-$Si_3N_4$ and γ-$Ge_3N_4$ using diamond anvil cell techniques were complemented by large volume press syntheses that allowed structure determination by Rietveld refinement of powder X-ray diffraction data (39, 40), and later led to preparation of γ-$(Si,Ge)_3N_4$ solid solutions and intermediate compounds (46). Synchrotron X-ray emission and absorption (XES/XAS) studies were combined with *ab initio* theoretical calculations to understand the ground and excited state electronic structures and evaluation of the bandgap properties (44, 45). Recent laboratory investigations of the optical properties of $Sn_3N_4$ are now revealing pressure-induced tuning of the bandgap between 1.3-3.0 eV under compression up to 100 GPa, leading to the possibility for controlling the optoelectronic properties *via* strain engineering (47). Attention later focused on mixed-anion oxynitride spinels in the Si-Al-O-N and Ga-O-N systems (48-51), using synchrotron XAS to characterise the local structure around the $Al^{3+}$ cations (52). In our work, we used a combination of laser-heated DAC and multianvil synthesis techniques to prepare $Ga_4O_3N$ samples that were characterised using Raman spectroscopy and synchrotron X-ray diffraction. Rietveld analysis of the angle-dispersive data showed a deficiency of Ga on the octahedral sites and O/N disorder on the anion sites (50). Experiments to further develop and understand the crystal chemistry of nitride and oxynitride spinels are now under way worldwide, using advanced synchrotron-based techniques to examine the structures and their optoelectronic properties (53).

Shortly after observation of the first nitride spinels, theoretical studies began to predict the possible occurrence of spinel-structured nitrides containing transition metal cations including Fe, Mn and Ti (54-56). Such materials are potentially important as the functional (e.g., magnetic, catalytic) properties of oxide spinels are mainly determined by the presence of transition metal ions within the structures. In the case of titanium nitride[4], it had been observed that polymerization of Ti alkylammonium precursors ($Ti(NMe_2)_4$ or $Ti(NEt_2)_4$) in liquid $NH_3$ yielded X-ray amorphous products with N-rich compositions $Ti_3(N,C)_4$ (57). In collaboration with the group of A. Hector in Southampton, we repeated these experiments and annealed the resulting compounds in $N_2$ atmospheres to produce amorphous to nanocrystalline solids with compositions near $Ti_3(C_{0.17}N_{0.78}H_{0.05})_{3.96}$. These were then studied using XAS/EXAFS techniques at Daresbury SRS (station 7.1) (58). The results showed that the Ti-N bond lengths corresponded to those expected for octahedrally bonded units, but with an initial average coordination number near 4.5, while the second-nearest neighbor coordination was approximately 5.5. These results indicated that the $Ti_3(N,C)_4$ compound produced was based on a defective NaCl-structured lattice, containing ~40% vacancies on the metal (Ti) sites and ~50% vacancies on the anion (N,C) sites. Continued annealing to above 700°C resulted in a gradual increase in the $TiN_6$ coordination number and a jump in the second neighbour coordination to ~12, associated with final densification into the rocksalt-structured TiN phase (58).

Laser-heated DAC studies then showed the formation of $Zr_3N_4$ and $Hf_3N_4$ with the cubic $Th_3N_4$ structure by direct combination between the elements under high-P,T conditions (59). In our work we explored the formation of additional dense $Hf_3N_4$ and $Ta_3N_5$ polymorphs by compressing and laser heating the amorphous/nanocrystaline precursors obtained from organometallic precursor reactions, using synchrotron XRD to identify the new phases formed and assign their structures (60, 61). Kroll had previously reported DFT calculations of the relative energetics of different $Ti_3N_4$, $Hf_3N_4$, $Zr_3N_4$ polymorphs as a function of pressure (62). In that work it was predicted that a "defective" NaCl-structured $Ti_3N_4$ phase should occur at highest energy, whereas the cubic $Th_3N_4$-structured phase should become stabilised above 15 GPa, while the spinel-structured form would remain metastable throughout the pressure range. A recent publication has now reported the high-P,T synthesis of $Ti_3N_4$ with the cubic $Th_3P_4$ structure formed by reacting TiN and $N_2$ in a laser heated DAC at ~75 GPa and 2400 K (63).

We investigated the transformation behavior of our amorphous to nanocrystalline $Ti_3(N,C)_4$ samples first at high pressure, and then following high-P,T treatment, using a combination of synchrotron XRD and Raman scattering. In an initial Raman study at ambient temperature, we observed that the very broad, weak features of the amorphous to nanocrystalline starting material evolved into broad bands that could be associated with acoustic phonon density of state signatures of the defective rocksalt structure. These then reverted to the

initial broad "amorphous" signal upon decompression (see Figure 4 in ref. (64)). In a second experiment, laser heating to 1000-1400K at 17.4 GPa in our UCL laboratory caused an additional Raman band to appear near 500 $cm^{-1}$ (64). However, synchrotron studies carried out at APS using a high power $Nd^{3+}$:YAG laser to heat the samples at 19 GPa found only XRD peaks for the rocksalt structured phase (64). Further results were reported in the PhD thesis of Dr. Ashkan Salamat (now at University of Nevada, Las Vegas) (65). $Ti_3(N,C)_4$ precursor samples were loaded into a DAC, pressurized to 17 GPa using $N_2$ as a pressure medium, and heated "gently" using a $CO_2$ laser ($\lambda$ = 10.6 μm) installed in our UCL laboratory (50, 66), using Raman spectroscopy to monitor the structural changes. Once the characteristic 500 $cm^{-1}$ band had appeared in the spectrum, the sample was transported to DLS (beamline I15) for a previously scheduled experiment (on-line DAC laser heating has only recently been installed at the beamline). The XRD pattern showed the appearance of 13 new crystalline peaks that could not be indexed to any single new phase (Fig. 2). While at the beamline, the pressure was increased to 28 GPa, but without further heating, prior to decompression at ambient T. The XRD pattern exhibited changes in the relative peak intensities, but no satisfactory structure solution could be obtained. It was apparent that a mixture of crystalline phases had been produced. As the sample was decompressed, several peaks disappeared until by 5.3 GPa only four main peaks remained with *d* spacings of 2.115, 2.446, 2.546 and 3.511 Å. After decompressing to 3.3 GPa these peaks began to develop weak shoulders that grew into separate reflections as final pressure release occurred (Fig. 2). These could indicate either structural distortion within the initial main phase, or else appearance of a different $Ti_3N_4$ polymorph. It is also important to note that the "4-peak" pattern that remains following decompression to below 9.5 GPa is actually present in the XRD data for the laser-heated material compressed at 17 GPa and above. Le Bail refinement of the XRD data for the material decompressed to ~3 GPa could be indexed within orthorhombic space group *Pmc2* with lattice parameters a=4.012 Å, *b*=3.513 Å, *c*=4.888 Å ($V_o$ = 68.873 $Å^3$: $R_{wp}$ 6.21). The pattern did not fit at all with that estimated for spinel-structured $Ti_3N_4$, and the refined cell volume is ~10% smaller than that of B1-structured TiN. (65). The peaks appearing near 9 and 12 °2θ could correspond to a rocksalt structured $Ti_3N_4$ phase, but the relative intensities are perturbed and additional peaks near 7 and 10.5 °2θ are not accounted for. These results highlight the need for further studies of the stable and metastable transformation behavior of stable and metastable nitride structures, using chemical precursor routes to achieve designed initial stoichiometries that can examined by high-P,T experiments at synchrotron beamlines.

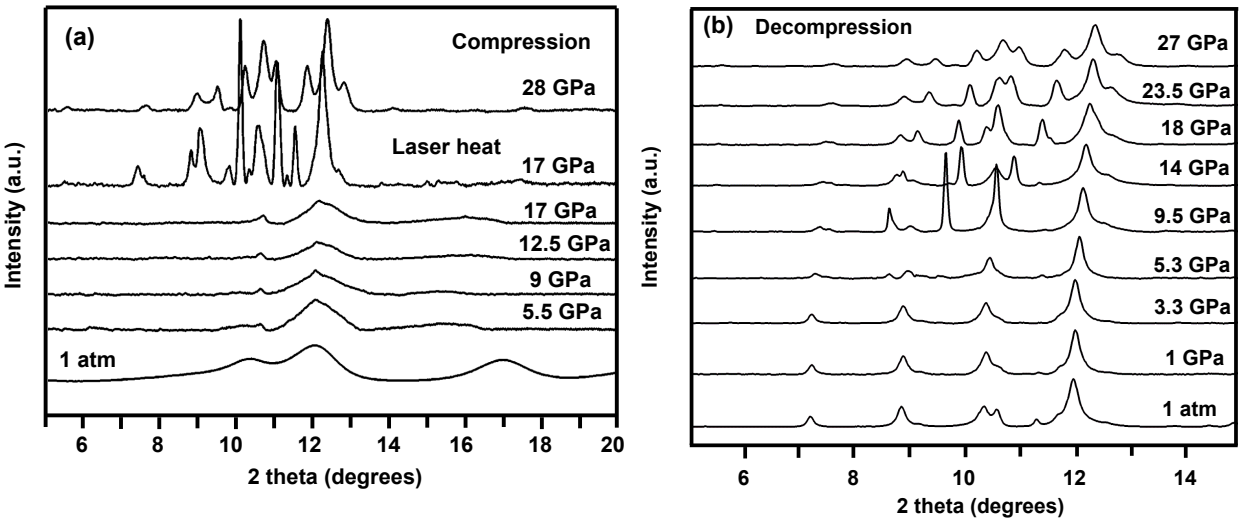


**Figure 2.** Results of compression and laser heating under high-P conditions of an amorphous to nanocrystalline $Ti_3(N,C)_4$ sample prepared from precursors (58, 64, 65). Left: synchrotron X-ray diffraction carried out at DLS I15 ($\lambda$ = 0.442110 Å) for an amorphous/nanocrystalline $Ti_3(N,C)_4$ sample at ambient T up to 17 GPa, and then following $CO_2$ laser heating at UCL at 17 GPa, and subsequently increasing the pressure to 28 GPa (Diagrams adapted from the PhD thesis of Ashkan Salamat, ref. (65)). Right: evolution of the synchrotron XRD pattern during decompression from 27 GPa to ambient for the recrystallised $Ti_3(N,C)_4$ sample following the laser heating experiment (65).

## High-Density Carbon Nitrides

Research into solid state and polymeric carbon nitride compounds began in the early to mid-1800's as chemists including Berzelius, Wohler and Liebig first sought to expand and establish the field of cyanogen chemistry(14, 67). The earliest studies concerned the thermal decomposition of $Hg(SCN)_2$ leading to an H-free phase predicted to have $C_3N_4$ stoichiometry. Liebig concentrated his initial studies on the corresponding isothiocyanate system containing $NH_4^+$ cations, and produced a range of polymeric solids with different $C_xN_yH_z$ compositions. His analyses revealed one compound with composition near $C_6N_9H$ that he named "melon", and this terminology was then applied to the series of materials designated "melem", "melamine" etc. (68). Discussions about the nature of these polymeric solids attracted the attention of chemists and crystallographers, including L. Pauling who first deduced that they should be based on the tri-*s*-triazine (heptazine, $C_6N_7$) core rather than simply linking together independent triazine ($C_3N_3$) ring units (69). The structure of Liebig's melon was only determined recently using a combination of spectroscopic, imaging, diffraction and computational techniques, to show that it indeed consisted of ribbon-like structures based on polyheptazine (PH) units linked by -NH- groups and containing terminal $-NH_2$ species that engaged in H-bonding between the PH chains (68).

The field attracted relatively little attention until the 1980's when it was predicted theoretically that an $sp^3$-bonded $C_3N_4$ phase initially suggested to have a $Si_3N_4$ structure would have low compressibility and potentially high hardness, potentially competitive with diamond (4, 5). That suggestion motivated many attempts to synthesize dense carbon nitrides, using chemical and physical vapour deposition (CVD) as well as HPHT techniques. However, that goal has still not been achieved. In collaboration with research teams in Darmstadt and Mainz (Germany), our group investigated laser heating the carbon nitride precursor dicyandiamide (DCDA, $C_2N_4H_4$) in a DAC (6). Below 27 GPa only a black amorphous product was found that was presumed to correspond to graphitisation of the sample, but above this pressure transparent regions containing crystalline Raman peaks were observed in those parts of the sample that had been laser heated to >1700°C (6). After decompression to ambient conditions a small number of single crystals could be extracted from the sample. Chemical analysis using a combination of TEM EELS and nano-SIMS showed the composition to be $C_2N_2H$, and electron diffraction. DFT results indicated a defective wurtzite (dwur) structure with tetrahedral sites occupied by $sp^3$-bonded C and N (Fig. 3). One empty C site was occupied by H that had moved off-centre to form an N-H bond. The crystalline compound could also be formulated as carbon nitride imide, $C_2N_2(NH)$, isostructural with $Si_2N_3(NH)$ and the mineral sinoite ($Si_2N_2O$), that were already well-known phases.

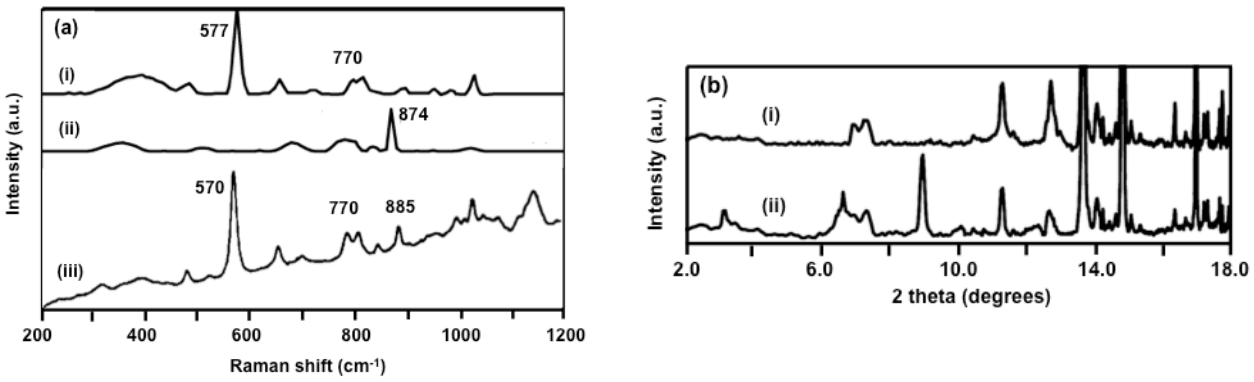


**Figure 3.** Evidence for new metastable phases formed in the C-N-H system under HPHT conditions. (a): Raman spectra obtained following laser heating (LH) $C_2N_2H_2$ in the DAC at 30-45 GPa to produce $C_2N_4H_4$. (i) Spectra obtained after extended LH are dominated by a strong peak at 570-580 $cm^{-1}$ due to the dwur-$C_2N_2H$ phase identified by DFT calculations (7). (ii) Spectra obtained after short periods of LH are instead dominated by a peak at 875-885 $cm^{-1}$ that does not appear in the dwur-$C_2N_2H$ spectrum. (iii) Spectra collected for intermediate heating periods contain both peaks, as reported in the original publication (6, 7, 65). In most cases a broad feature is observed in the 300-400 $cm^{-1}$ region that we assign to amorphous C-N-H material that did not fully crystallised during the HPHT synthesis experiment. (b) Synchrotron XRD data collected following LH-DAC synthesis of dwur-$C_2N_2H$ at 40 GPa. (i) Data collected following extended LH shows the expected reflections for the dwur-$C_2N_2H$ phase. (ii) Data collected after a short LH period contains additional diffraction lines indicating formation of an intermediate crystalline phase (65).

We made several attempts to study this material formed under HPHT conditions using XRD at Daresbury SRS, but the presence of only light elements within this phase made the task difficult during the beamtime available at the 2G synchrotron light source (70). However, later X-ray experiments at Diamond I15 and at the ESRF (ID27) proved successful (7). These studies importantly demonstrated that the reaction proceeded *via* loss of $NH_3$ component from the $C_2N_4H_4$ precursor, both by recording XRD from the condensed solid at high pressure, and observation of a bubble formed during the last stages of decompression, that escaped from the cell during pressure release (7, 65). The diffraction pattern corresponded to that of the *Cmc2*$_1$ structure established from the recovered phase and DFT calculations in the previous study. Our new work permitted us to establish that no structural transformations occurred during decompression and also provided bulk modulus parameters for the new dwur-$C_2N_3H$ phase (7). The dwur-structured $C_2N_3H$ phase remains the only fully $sp^3$-bonded carbon nitride structure that has been properly established to date.

Our laboratory-based spectroscopic and synchrotron X-ray studies also allowed us to observe that additional stable or metastable $C_3N_y$ or $C_xN_yH_z$ crystalline phases must be present within the system (Fig. 3). In our initial Raman data obtained at UCL and MPI Mainz, we observed sharp peaks at 577 and 874 $cm^{-1}$ along with a broader asymmetric band at 770 $cm^{-1}$, that showed variable intensity between different runs (6). We suggested that this likely indicated a transient metastable structure formed during polymerisation of the $C_2N_4H_4$ precursor. In subsequent work, we also determined that the 577 and 874 $cm^{-1}$ peaks correspond to two different phases, because their relative intensities varied systematically with the duration of LH-DAC heating runs (7, 65). Sychrotron X-ray diffraction indicated three peaks near 3.2, 6.4 and 9 °2θ ($\lambda$ = 0.26473 Å) that could correspond to a new phase, that has not yet been identified. *Ab initio* random structure searching (AIRSS) calculations carried out in collaboration with Prof. Chris Pickard (Cambridge) have revealed that the C-N-H system is rich in potential structural polymorphs that might be produced stably or metastably during such HPHT experiments, that provide interesting targets for future experimental and computational studies (71).

## Compression Studies of Layered Carbon Nitrides

By analogy with the phase diagram of pure carbon, $sp^2$-bonded graphitic forms of $C_3N_4$ were expected to form the most stable structures at ambient pressure. These were first modelled as polytriazine motifs with $C_3N_3$ rings linked by -N= units to form planar sheets related to what later became recognised as "graphene", containing $C_6N_6$ ring voids (5, 72, 73). Such a structure was proposed for the nanocrystalline materials prepared as thin films by CVD methods, and demonstrated to have $C_3N_4$ stoichiometry (74). A bulk crystalline variety of this graphitic phase was recently described by Algara-Siller et al. (75).

Zhang et al. first prepared a new type of carbon nitride layered structure, by condensing melamine and cyanuric chloride under HPHT conditions (P=1-1.5-2 GPa; 500-600°C) to form a yellow crystalline solid. The composition was determined to be $C_6N_9H_3$.HCl (76). The structure was determined to consist of planar layers with $C_6N_9H_3$ (i.e., $C_2N_3H$, as found for both Liebig's melon and the $sp^3$-bonded dwur structure described above) composition. The graphene-like sheets contained larger ($C_{12}N_{12}$) voids than for the $C_3N_4$ polytriazine model described above, with -(NH)- units bridging between the $C_3N_3$ rings. The $Cl^-$ ions were located within the large $C_{12}N_{12}$ rings, and the additional protons were accomodated by bonding to adjacent N atoms of the triazine rings (76-78). The behaviour of this material at high pressure was studied by synchrotron XRD in the diamond anvil cell, beginning with initial studies at Daresbury SRS (64, 70) and then at ESRF (ID27) and DLS (I15) (8). The interlayer (002) reflection shifted rapidly to small *d* spacing values during initial compression, as expected for a layered solid. Above 10 GPa the diffraction peaks became broadened but remained recognisable up to 36 GPa. However, by 40 GPa changed significantly to become dominated by a broad asymmetric feature at ~13 °2θ ($\lambda$ = 0.3738 Å) (8). Carrying out DFT calculations allowed us to interpret these structural changes. Between 10-20 GPa, the initially flat carbon nitride layers buckle around the -(NH)- linkage sites acting as "hinge" positions, and the $Cl^-$ ions are displaced along the original *c* axis towards previously interlayer sites. By approximately 40 GPa, a structure containing C-N bonds between atoms that were previously in adjacent layers begins to become stabilised. Within the periodic boundary conditions applied for the DFT calculations, this resulted in formation of $sp^3$-hybridised C,N "nanotubes" running throughout the structure, linked laterally by $sp^2$-bonded ring units (Fig. 4) (8). This result is linked to recent interest in C- and C,N-based "nanothreads" produced from organic molecular precursors under high-P conditions (79, 80). In our experiments, the broadened diffraction features indicates that the interlayer bonding occurred in a random fashion (8).

In our preliminary experiments, a $C_6N_9H_3$.HCl sample was loaded into a DAC using NaCl as a pressure transmitting medium (PTM), compressed to 30 GPa and heated at UCL using a $CO_2$ laser. The loaded DAC was then transported to ESRF ID27 for XRD examination. The laser heating had resulted in a series of crystalline peaks appearing (Fig. 4). To confirm the results, a second sample was loaded with LiF as PTM and

heated at the beamline using $Nd^{3+}$:YAG laser excitation with a small quantity of Re powder added to the sample to act as an absorber of the near-IR radiation (70, 81). Laser heating a sample compressed to 30 GPa resulted in appearance of sharp crystalline peaks (Fig. 4). The results did not correspond to the diffraction pattern expected for the pillared-layered phase predicted using DFT calculations at high pressure, but some similarities emerged as the sample was decompressed to ambient pressure. Initial attempts to find a structural solution were described in the PhD thesis of A. Salamat (65). These preliminary results indicate fertile ground for future studies combining LH-DAC and synchrotron XRD studies.

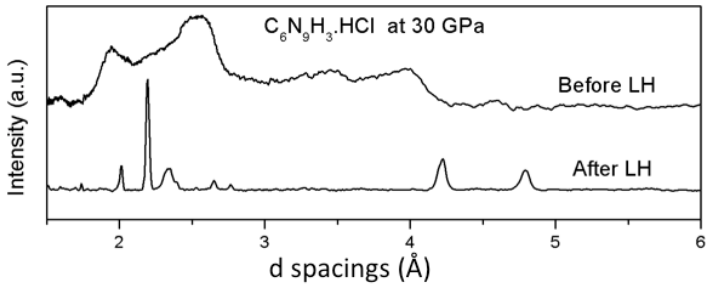


**Figure 4.** XRD patterns of $C_6N_9H_3$.HCl compressed to 30 GPa before and after laser heating (65). Peaks due to the NaCl PTM have been removed (65).

In more recent work, we examined the high pressure transformation behaviour of graphitic carbon nitride with a crystalline triazine based g-$C_3N_4$ structure (TGCN) described by Algara-Siller et al (75). A sample flake was loaded into a DAC using Ne as the pressure-transmitting medium, compressed to 53 GPa where the initial graphitic peaks had broadened and disappeared, while monitoring the structural changes using synchrotron XRD at ESRF ID27 during $CO_2$ laser heating experiments (10, 82, 83). After heating, the pressure was found to have decreased to 44 GPa and a series of crystalline diffraction peaks appeared. These could not be indexed to any of the predicted dense $C_3N_4$ phases. However, in a parallel series of AIRSS calculations designed to sample and study the relative stabilities of different stable and metastable $C_3N_4$ structures across a wide range of high-P regimes, it was predicted that new open-framework phases based on mixed $sp^2$-$sp^3$ bonded units might exist, that might even be competitive with the graphitic layered structures at ambient P,T conditions (10). We tested these potential structures and their predicted diffraction patterns against the observed data, and found a match to the series of *d* spacings observed in the compound recovered to ambient conditions. The relative intensities did not correspond between the predicted and observed patterns, but we noted that the experimental data consisted of diffraction spots from a few crystalline regions contained within the sample, rather than a powder average. The best fit structure had orthorhombic symmetry within a $P4_12_12$ (or $P4_32_12$) space group, and contained triazine ring units linked into a 3D framework structure by $sp^3$ bonded C atoms (10). This constitutes a new structure type within the C-N system, that deserves further study. In very recent studies, methods similar to those used by Algara-Siller et al to obtain the TGCN-structured g-$C_3N_4$ used as a precursor for our HPHT synthesis studies were shown to give rise to more C-rich graphitic layered materials, with compositions between $C_3N_4$ and $C_4N_3$ (84, 85). Taken together with the additional structures suggested by our work on the $C_2N_3H$ composition described above, these observations indicate new areas for further exploration using advanced synchrotron-based techniques combined with laboratory experiments and *ab initio* theoretical investigations.

## Layered Carbon Nitrides for Functional Applications

Layered to polymeric materials in the C-N and C-N-H systems combine several useful properties including their wide-gap semiconducting nature, with a bandgap extending into the visible region that straddles the $H^+/H_2$ and $O_2/H_2O$ redox potentials for water splitting, the availability of exchangeable protons as N-H species, and lone pairs located on the N atoms. These functionalities are being investigated for applications ranging from catalysis and photocatalysis, to possibilities for electronic and ionic charge storage, and for providing active tethering sites for catalytic metal nanoparticles (14). In addition, certain materials exhibit an unpaired electron signature leading to possibilities for information storage, as well as unusual magnetic properties (85). In recent work supported by the EPSRC and the EU Graphene Flagship our group has been investigating the electrochemical properties of functionalised carbon nitrides and graphene samples as catalyst supports for PEM fuel cells and electrolysers (11, 12, 15), and have been developing *operando* X-ray absorption measurements during electrochemical test studies at the new dispersive XAS beamline (I20-EDE)

at Diamond, in collaboration with DLS researchers and the group of Prof. Andrea Russell at Southampton University (R. Jervis, A. Leach et al., in prep).

## Exfoliation and Dissolution of Low-Dimensional Carbon Nitrides

As an important class of layered solids, there has been interest in studying their exfoliation to produce single- to few-layered 2D nanomaterials related to graphene, but with wide-gap semiconducting properties and added chemical functionality (ref?? Bojdys 2013). Most studies have investigated mechanical or chemical exfoliation in the presence of a liquid phase, to create colloidal suspensions or true solutions containing the 2D species (Coleman 2013; Cullen Nat Chem 2016). Small angle neutron scattering (SANS) has been used to establish the nature of C "nanotubide" and graphenide anions in solution following framework charging and exfoliation (ref?? C Howard ACS Nano 2012; other refs?). We recently observed the spontaneous exfoliation and dissolution of layered carbon nitrides with a polytriazine imide (PTI) structure containing intercalated $Li^+$ and $Cl^-$ or $Br^-$ species when placed in contact with polar liquids including DMF, DMSO and NMP without exchangeable protons (16, 17). Other studies in $H_2O$ indicate $H^+/Li^+$ exchange between the PTI solid and the solvent resulting in pH changes (17, 86). We are currently engaged in combined neutron and high-energy synchrotron X-ray scattering experiments to establish the nature of the dissolved species, and their effects on the surrounding solvent (M.C. Wilding, C.A. Howard, PFM et al., in prep.).

## Summary and Conclusions

Our synchrotron studies of HP-HT synthesis and physical properties of new nitride materials have revealed a series of interesting structures and reaction pathways, and have also pointed towards a rich variety of stable and metastable structure types with potentially useful properties that should be explored in future investigations. Areas that deserve further attention include both metallic and high oxidation state transition metal nitrides and carbonitrides, as well as main group semiconducting nitrides and new dense framework structures based on the light elements C-N-O. In our more recent work, synchrotron X-ray spectroscopy is contributing to new understanding of the oxidation state changes and interactions between catalytic metal nanoparticles and light element supporting materials that occur during electrochemical processes, important for energy storage and conversion devices. In addition, synchrotron X-ray combined with neutron scattering is leading to new insights into the nature and solvation mechanisms of low-dimensional nanomaterials prepared by spontaneous exfoliation and dissolution processes.

**Acknowledgments**
The studies described here include contributions from several former PhD students as well as post doctoral researchers and colleagues. Preliminary results have been presented in PhD theses and are cited here. These represent areas for future development and research that should be pursued at next-generation synchrotron sources.

**Funding Statement**
Our high pressure-high temperature studies to explore new nitrides as well as other systems under HPHT conditions has been supported by EPSRC as well as a Wolfson-Royal Society Research Merit Award. Our recent work on functional carbon nitride materials and exfoliation/dissolution studies have been funded by EPSRC grant EP/L017091 and by the EU Graphene Flagship under Horizon 2020 research and innovation grant agreement No. 696656 - Graphene Core 1.

**Competing Interests**
The author declares no competing interests.

## References

1. Salamat A, Hector AL, Kroll P, McMillan PF. 2013. *Coord Chem Rev*. **257**,2063-72.
2. Kinski I, McMillan PF. Gallium nitrides and oxonitrides. In: Riedel R, Chen I-W, editors. Ceramics Science and Technology, vol 2, Materials and Properties. Weinheim, Germany: Wiley-VCH; 2010.
3. Horvath-Bordon E, Riedel R, Zerr A, McMillan PF, Auffermann G, Prots Y, Kniep R, Kroll P. 2006. *Chem Soc Rev*. **35**,987-1014.
4. Cohen ML, Liu AY. 1989. *Science*. **245**,841-2.
5. Teter D, Hemley RJ. 1996. *Science*. **271**

6. Horvath-Bordon E, Riedel R, McMillan PF, Kroll P, Miehe G, van Aken P, Zerr A, Hoppe P, Shebanova O, McLaren I, Lauterbach S, Kroke E, Boehler R. 2007. *Angew Chem Int Ed*. **46**,1476-80.
7. Salamat A, Woodhead K, McMillan PF, Quesada Cabrera R, Perrillat J-P, Rahman A, Adriens D, Corà F. 2009. *Phys Rev B*. **80**,104106.
8. Salamat A, Deifallah M, Quesada Cabrera R, Corà F, McMillan PF. 2013. *Sci Rep*. **3**,2122.
9. Pickard CJ, Needs RJ. 2011. *J Phys Cond Matter*. **23**,053201.
10. Pickard CJ, Salamat A, Bojdys MJ, Needs RJ, McMillan PF. 2016. *Phys Rev B*. **94**,094104.
11. Mansor N, Jorge AB, Corà F, Gibbs C, Jervis R, McMillan PF, Wang X, Brett DJL. 2014. *J Phys Chem C*. **118**,6831-8.
12. Mansor N, Miller TS, Dedigama I, Jorge AB, Jia J, Brázdová V, Mattevi C, Gibbs C, Hodgson D, Shearing PR, Howard CA, Corà F, Shaffer M, Brett DJL, McMillan PF. 2016. *Electrochim Acta*. **222**,44-57.
13. Veith GM, Baggetto L, Adamczyk LA, Guo B, Brown SS, Sun X-G, Albert AA, Humble JR, Barnes CE, Bojdys MJ, Dai S, Dudney NJ. 2013. *Chem Mater*. **25**,503-8.
14. Miller TS, Jorge AB, Suter TM, Sella A, Corà F, McMillan PF. 2017. *Phys Chem Chem Phys*. **19**,15613-38.
15. Jia J, White ER, Clancy AJ, Rubio Carrero N, Suter TM, Miller TS, McMillan PF, Brazdova V, Corà F, Howard CA, Mattevi C, Shaffer MSP. 2018. *Angew Chem*.12838-42.
16. Miller TS, Suter TM, Telford AM, Picco L, Payton OD, Russell-Pavier F, Cullen PL, Sella A, Shaffer MSP, Nelson J, Tileki V, McMillan PF, Howard CA. 2017. *Nano Letts*. **17**,5891-6.
17. Suter TM. *Crystalline Carbon Nitrides: Characterisation, Intercalation and Exfoliation*, PhD thesis, University College London, 2017.
18. Fromme P. 2015. *Nature Chem Biol*. **11**,895-9.
19. Zhang C, Graves WS, Holl MR, Malin LE, Nanni EA, editors. Electron beam optics for the ASU compact XFEL. 9th Int Particle Accelerator Conf; 2018; Vancouver, Canada.
20. Gruner F, Becker S, Schramm U, Eichner T, Fuchs M, Weingartner R, Habs D, Meyer-ter-Vehn J, Geissler M, Ferrario M, Serafini L, Van der Geer B, Backe H, Lauth W, Reiche S. 2007. *Appl Phys B*. **86**,431-5.
21. Elsaesser T, Woerner M. 2014. *J Chem Phys*. **140**,020901.
22. H SJC, Weierstall U, Chapman HN. 2012. *Rep Prog Phys*. **75**,102601.
23. Turner JJ, Dakovski GL, Hoffmann MC, Hwang HY, Zarem A, Schlotter WF, Moeller S, Minitti MP, Staub U, Johnson S, S M, Swiggers M, Noonan P, Curiel GI, Holmes M. 2015. *J Synchrotron Rad*. **22**,621-5.
24. Seddon EA, Clarke JA, Dunning DJ, Masciovecchio C, Milne CJ, Parmigiani F, Rugg D, Spence JCH, Thompson NR, Ueda K, Vinko SM, Wark JS, Wurth W. 2017. *Rep Prog Phys*. **80**,115901.
25. Spence JCH. 2017. *IUCrJ*. **4**,322-39.
26. Bailey E, McMillan PF. 2010. *J Mater Chem*. **20**,4176-82.
27. Bull CL, Kawashima T, McMillan PF, Machon D, Daisenberger D, Soignard E, Takayama-Muromachi E, Chapon LC. 2006. *J Solid State Chem*. **179**,1761-6.
28. Machon D, Daisenberger D, Soignard E, Shen G, Kawashima T, McMillan PF. 2006. *phys stat solidi (a)*. **203**,831-6.
29. Kawashima T, Takayama-Muromachi E, McMillan PF. 2007. *Physica C*. **460-462**,651-2.
30. Wang S, Antonio D, Yu X, Zhang J, Cornelius AL, He D, Zhao Y. 2015. *Sci Rep*. **51**,13733.
31. Bull CL, McMillan PF, Soignard E, Leinenweber K. 2004. *J Solid State Chem*. **177**
32. Wang S, Ge H, Sun S, Zhang J, Liu F, Wen X, Yu X, Wang L, Zhang Y, Xu H, Neuefeind J, Qin Z, Chen C, Jin C, Li Y, He D, Zhao Y. 2019. *J Am Chem Soc*.
33. Soignard E, Shebanova O, McMillan PF. 2007. *Phys Rev B*. **75**,014104.
34. Shebanova O, McMillan PF, Soignard E. 2006. *High Press Res*. **26**,87-97.
35. Woodhead K, Pascarelli S, Hector AL, Briggs R, Alderman N, McMillan PF. 2014. *Dalton Trans*. **43**,9647-54.
36. Salamat A, Briggs R, Bouvier P, Petitgirard S, Dewaele A, Garbarino G, Daisenberger D, Cutler M, Corà F, McMillan PF. 2013. *Phys Rev B*. **88**,104104.
37. Woodhead KE. *High Pressure Polymorphism of Tantalum Nitrides and Oxynitrides*, PhD thesis, University College London, 2012.
38. Pascarelli S, Mathon O, Munoz M, Mairs T, Susini J. 2006. *J Synchrotron Rad*. **13**,351-8.
39. Leinenweber K, O'Keeffe M, Somayazulu M, Hubert H, McMillan PF, Wolf GH. 1999. *Chem Eur J*. **5**,3076.
40. Zerr A, Miehe G, Serghiou G, Schwarz M, Kroke E, Riedel R, Fueβ H, Kroll P, Boehler R. 1999. *Nature*. **400**
41. Scotti N, Kockelmann W, Senker J, Trabel S, Jacobs H. 1999. *Z Anorg Allg Chem*. **625**,1435-9.
42. Shemkunas MP, Wolf GH, Leinenweber K, Petuskey WT. 2002. *J Am Ceram Soc*. **86**,101-4.
43. Dong J, Deslippe J, Sankey OF, Soignard E, McMillan PF. 2003. *Phys Rev B*. **67**,094104.
44. Boyko T, Moewes A, Bailey E, McMillan PF. 2010. *Phys Rev B*. **81**,155207.
45. Boyko T, Hunt A, Zerr A, Moewes A. 2013. *Phys Rev Lett*. **111**,097402.
46. Soignard E, Somayazulu M, Mao H-k, Dong J, Sankey OF, McMillan PF. 2001. *Solid State Commun*. **120**,237-42.
47. Kearney JSC, Grauzinte M, Smith D, Sneed D, Childs C, Hinton J, Park C, Smith JS, Kim E, Fitch SDS, Hector AL, Pickard CJ, Flores-Livas JA, Salamat A. 2018. *Angew Chem Int Ed*. **57**,11623-8.
48. Kinski I, Miehe G, Heymann G, Theissmann R, Riedel R, Huppertz H. 2005. *Z Naturforsch*. **60b**,832-6.
49. Kinski I, Scheiba F, Riedel R. 2005. *Adv Eng Mater*. **7**,921-7.

50. Soignard E, Machon D, McMillan PF, Dong J, Xu B, Leinenweber K. 2005. *Chem Mater*. **17**,5465-72.
51. Schwarz M, Zerr A, Kroke E, Miehe G, Chen I-W, Heck M, Thybush B, Poe BT, Riedel R. 2002. *Angew Chem Int Ed*. **41**,789-93.
52. Tatsumi K, Mizoguchi T, Yoshioka S, Yamamoto T, Suga T, Sekine T, Tanaka I. 2005. *Phys Rev B*. **71**,033202.
53. Nishiyama N, Ishikawa R, Ohfuji H, Marquardt H, Kurnosov A, Taniguchi T, Kim B-N, Yoshida H, Masuno A, Bednarcik J, Kulik E, Ikuhara Y, Wakai F, Irifune T. 2017. *Sci Rep*. **7**,44755.
54. Ching WY, Mo S-D, Ouyang L, Tanaka I, Yoshiya M. 2000. *Phys Rev B*. **61**,10609.
55. Ching WY, Mo S-D, Tanaka I, Yoshiya M. 2001. *Phys Rev B*. **63**,064102.
56. Ching WY, Xu Y-N, Rulis P. 2002. *Appl Phys Lett*. **80**,2904.
57. Baxter DV, Chisholm MH, Gama GJ, Hector AL, Parkin IP. 1996. *Chem Mater*. **8**,1222-8.
58. Jackson AW, Shebanova O, Hector AL, McMillan PF. 2006. *J Solid State Chem*. **179**,1383-93.
59. Zerr A, Miehe G, Riedel R. 2003. *Nature Mater*. **2**,185-9.
60. Salamat A, Hector AL, Gray BM, Kimber SAJ, Bouvier P, McMillan PF. 2013. *J Am Chem Soc*. **135**,9503-11.
61. Salamat A, Woodhead K, Shah S, Hector A, McMillan PF. 2014. *Chem Commun*. **50**,10041-4.
62. Kroll P. 2003. *Phys Rev Lett*. **90**,125501.
63. Bhadram VS, Liu H, Xu E, Li T, Prakapenka VB, Hrubiak R, Lany S, Strobel TA. 2018. *Phys Rev Mater*. **2**,011602.
64. McMillan PF, Shebanova O, Daisenberger D, Quesada Cabrera R, Bailey E, Hector A, Lees V, Machon D, Sella A, Wilson M. 2007. *Phase Transitions*. **80**,1003-32.
65. Salamat A. *High Pressure Solid State Chemistry of C-N-H and Ti-N Systems*, PhD thesis, University College London, 2009.
66. Soignard E. *High Pressure - High Temperature Synthesis and Studies of Nitride Materials*, PhD thesis, University College London, 2003.
67. Miller TS, d'Aleo A, Suter TM, Aliev AE, Sella A, McMillan PF. 2017. *Z Anorg Allg Chem*. **643**,1572-80.
68. Lotsch BV, Döblinger M, Sehnert J, Seyfarth L, Senker J, Oeckler O, Schnick W. 2007. *Chem Eur J*. **13**,4969-80.
69. Pauling L, Sturdivant JH. 1937. *Proc National Acad SciU SA*. **23**,615-20.
70. Lees VJ. *High Pressure Synthesis and Characterisation of Layered Carbon Nitride Materials*, PhD thesis, University College London, 2009.
71. Rahman A. *Theoretical and Experimental Investigations of Graphitic and Crystalline Carbon Nitrides*, PhD thesis, University College London, 2014.
72. Ortega J, Sankey OF. 1995. *Phys Rev B*. **51**,2624-7.
73. Lowther JE. 1999. *Phys Rev B*. **59**,11683-6.
74. Kouvetakis J, Todd M, Wilkens B, Bandari A, Cave N. 1994. *Chemistry of Materials*. **6**,811-4.
75. Algara-Siller G, Severin N, Chong SY, Björkman T, Palgrave RG, Laybourn A, Antonietti M, Khimyak YZ, Krasheninnikov AV, Rabe JP, Kaiser U, Cooper AI, Thomas A, Bojdys MJ. 2014. *Ang Chem Int Ed*. **53**,7450-5.
76. Zhang Z, Leinenweber K, Bauer M, Garvie LAJ, McMillan PF, Wolf GH. 2001. *J Am Chem Soc*. **123**,7788-96.
77. Deifallah M, McMillan PF, Corà F. 2008. *J Phys Chem C*. **112**,5447-53.
78. McMillan PF, Lees V, Quirico E, Montagnac G, Sella A, Reynard B, Simon P, Deifallah M, Corà F. 2009. *J Solid State Chem*. **182**,2535-42.
79. Fitzgibbons TC, Guthrie M, Xu E-s, Crespi VH, Davidowski SK, Cody GD, Alem N, Badding JV. 2014. *Nature Mater*. **14**,43-7.
80. Li X, Wang T, Duan P, Baldini M, Huang H-T, Chen B, Juhl SJ, Koeplinger D, Crespi VH, Schmidt-Rohr K, Hoffmann R, Alem N, Guthrie M, Zhang X, Badding JV. 2018. *J Am Chem Soc*. **140**,4969-72.
81. McMillan PF, Lees V, Quirico E, Montagnac G, Sella A, Reynard B, Simon P, Bailey E, Deifallah M, Corà F. 2009. *J Solid State Chem*. **182**,2670-7.
82. Petitgirard S, Salamat A, Beck P, Weck G, Bouvier P. 2014. *J Synchrotron Rad*. **21**,89-96.
83. Salamat A, Fischer RA, Briggs R, McMahon MI, Petitgirard S. 2014. *Coord Chem Rev*. **277-278**,15-30.
84. Ladva SA, Travis W, Quesada-Cabrera R, Rosillo-Lopez M, Afandi A, Li Y, Jackman RB, Bear JC, Parkin IP, Blackman C, Palgrave RG. 2017. *Nanoscale*. **9**,16586-90.
85. Suter TM, Brázdová V, Miller TS, Nagashima H, Salvadori E, McColl K, Cockcroft JK, Vickers M, Sella A, Howard CWM, Corà F, McMillan PF. 2018. *J Phys Chem C*. **122**,25183-94.
86. Schwinghammer K, Mesch MB, Duppel V, Ziegler C, Senker J, Lotsch BV. 2014. *J Am Chem Soc*. **136**,1730-3.